THE EFFECTIVE-THICKNESS CONCEPT IN LAMINATED-GLASS ELEMENTS UNDER STATIC LOADING

M. López-Aenlle[a], F. Pelayo[a*], A. Fernández-Canteli[a] and M. A. García Prieto[a]

[a]Department of Construction and Manufacturing Engineering, University of Oviedo, Campus de Gijón, Zona Oeste, Edificio 7, 33203, Gijón, Spain.

[*]corresponding author; E-mail: fernandezpelayo@uniovi.es phone:+34 985182057

ABSTRACT: Laminated glass is a sandwich element consisting of two or more glass sheets, with one or more interlayers of a polymer such as polyvinyl butyral (PVB). The static response of sandwich elements such as laminated-glass beams and plates can be modeled using analytical or numerical models in which the glass is usually modeled as linear-elastic and the PVB as linear-viscoelastic material, respectively. As a way to simplify the laminated-glass calculations, the concept of effective thickness has been recently proposed, which allows the calculation of laminated-glass beams as monolithic beams using an apparent or effective thickness. In this work, equations for the effective thickness of laminated-glass beams are derived from the analytical model proposed by Koutsawa and Daya and the results provided by this model are compared with the models of Bennison et al. and Galuppi and Royer-Carfagni. Finally, some static experimental tests were performed on several laminated-glass beams under distributed loading in order to validate the predictions of the models.

Keywords: glass; viscoelastic; laminated; beams.

NOMENCLATURE

CAPITAL LETTERS

C_1, C_2	Coefficients of the WLF time-temperature superposition model
E	Young's Modulus
EI^*	Effective stiffness
$E_2(t)$	Viscoelastic relaxation tensile modulus for PVB
E_0	Glassy tensile modulus
$G_2(t)$	Viscoelastic relaxation shear modulus for PVB
G_0	Glassy shear modulus
H_1	Thickness of glass layer 1 in laminated glass
H_2	Thickness of polymeric layer in laminated glass
H_3	Thickness of glass layer 3 in laminated glass
H_w	Deflection-effective thickness
H_σ	Stress-effective thickness
I	Second moment of area
$K(t)$	Viscoelastic bulk modulus
K_R	Rotational spring stiffness (Koutsawa and Daya model)
K_T	Translational spring stiffness (Koutsawa and Daya model)
L	Length of a glass beam
PVB	Polyvinyl butyral

T Temperature

T_0 Reference temperature

LOWERCASE LETTERS

a_T Shift factor (WLF time-temperature superposition model)

b Width of a glass beam

e_i Modulus coefficient in Prony's series viscoelastic model

t Time

1 INTRODUCTION

In recent years, the use of laminated glass in buildings has increased considerably, mainly in facades, roofs, stairs, and windows. Laminated glass consists of two or more sheets of monolithic glass with one or more interlayers of a polymer such as polyvinyl butyral (PVB). The thickness of the PVB layer is usually 0.38 mm or a multiple of this value. The adherence of the glass and PVB layers is provided by subjecting the shaped laminate to high temperature and pressure conditions in an autoclave.

The main advantage of laminated glass compared with monolithic glass is the safety provided in case of breakage, because the interlayer holds the fragments together by adhering to the PVB layer, reducing the injury risk. Moreover, the PVB interlayer considerably increases the damping, reducing the magnitude of the vibrations due to dynamic loadings.

Glass mechanical behavior is usually modeled as linear-elastic material but high scatter is expected in the mechanical strength because of the superficial micro-defects coming from the manufacturing process and subsequent manipulation. On the other hand, PVB is an amorphous thermoplastic which shows linear-viscoelastic behavior. A fundamental characteristic of viscoelastic materials is that the mechanical properties are frequency (or time) and temperature dependent. As the tensile modulus of the PVB is far less compared with that corresponding to glass, significant transverse shear appears in the viscoelastic layer [1, 2]

The glass mechanical properties are usually determined by static bending tests whereas those of the PVB are established by relaxation or creep tests in the time domain or its corresponding dynamic tests in the frequency domain [3, 4, 5]

Thus, the mechanical behavior of laminated glass is not elastic and the sections do not behave according to the Euler-Bernoulli Beam theory assumptions (plane sections remain plane) because the effect of shear strain cannot be neglected. This makes the structural analysis of laminated-glass elements more difficult.

The first studies on the bending of simply supported laminated-glass beams were conducted by: Hooper [6], who developed a mathematical model for bending under four-point loading; Behr et al. [7], who performed experimental tests on monolithic and laminated-glass beams; Edel [8], who studied the temperature effect on laminated glass; and Norville [9], who developed a simple multilayer model.

Asik and Tezcan [10] formulated three coupled non-linear differential equations for analyzing laminated-glass beams, these equations being valid for beams with different boundary conditions. An analytical solution to the differential equations is presented for the case of simply supported beams but the finite-difference method was used for the case of fixed supported beams because of the difficulty in finding an analytical solution. These researchers proved analytically that the behavior can be linear or non-linear, depending on the boundary conditions. Thus, in simply supported laminated-glass beams the behavior is linear, even for large deflections. On the other hand, beams with fixed ends show non-linear behavior, meaning that the effect of membrane stress should be considered.

Ivanov [11] formulated a simple mathematical model for triplex-glass beams (glass+PVB+glass) where the simple bending theory is applicable for the single glass layers and the interaction caused by the shear of the PVB-interlayer is described by an additional differential equation. The analytical solutions are provided for simply supported glass beams under uniform transverse load, which are used in an optimization process for determining the thickness of the different layers in order to provide a lightweight structure. The author concludes that, for lightweight structural design, the inner glass layer of laminated glass under external pressure should be thinner than the external glass layer.

On the other hand, Koutsawa and Daya [2] derived a mathematical model for the displacement, strain and stress fields of laminated glass beams on viscoelastic supports, which are modeled by two springs (rotational, K_R, and translational, K_T), at each end of the beam. The model is validated for the case

of the simply supported beam, which is a particular case of the general model, assigning $K_R = 0$ and $K_T = \infty$.

Bennison et al. [12] Calderone et al. [13] proposed the concept of effective thickness for simplifying calculations of laminated-glass elements, which is based on the analysis of composite sandwich structures originally developed by Wölfel [14]. This method consists of calculating the thickness of a monolithic beam for which the bending stiffness is equivalent to that of a laminated beam. Once the effective thickness is known, the displacements, stresses, and strains are calculated using the classical equations of the Euler-Bernoulli monolithic beam.

Recently Galuppi and Royer-Carfagni have proposed new simple equations for the deflection- and stress-effective thicknesses of laminated-glass beams with different loading and boundary conditions [15], called “enhanced effective thickness”. Using a variational approach to the problem, and assuming as shape functions the elastic deflection of the monolithic beam with the same loading and boundary conditions, the authors deduced new simple expressions for the effective thickness. The predictions of this approach are compared with the results provided by a finite-element model and with equations of the model of Bennison et al. [12]. According to the authors, the enhanced effective-thickness approach presents no additional difficulty with respect to the Bennison et al. formulation and, moreover, gives much better results when the beam is not simply supported and the load is not uniform. Later, the same authors [16] have extended this approach to laminated-glass plates, using the same assumptions as those considered for the laminated-glass beams.

The main equations for the effective thickness derived by Galuppi and Royer-Carfagni for laminated-glass beams [15] and plates [16] have been summarized in [17]. As a means of facilitating the application of the technique, the values of the coupling parameter ψ, have been tabulated for most of the cases relevant for the practical application.

In this paper, the exact equations for the apparent effective bending stiffness and the effective thickness of laminated-glass beams, are derived from the mathematical model developed by Koutsawa and Daya [2] and compared with the predictions provided by the models of Bennison et al. [12] and Galuppi and Royer-Carfagni [15]. Moreover, static tests were performed on four laminated-glass beams with different lengths and thicknesses, simply supported and with three supports, under distributed loading. The elastic properties of the glass and the viscoelastic properties of PVB were determined by static and relaxation tests carried out on glass and PVB specimens. Finally, the experimental results are compared with the predictions of Galuppi and Royer-Carfagni [15], Koutsawa and Daya [2], and Bennison et al. [12].

2 VISCOELASTIC BEHAVIOR

Polyvinyl butyral (PVB) can be considered a linear-viscoelastic material with mechanical properties that are frequency (or time) and temperature dependent [14].

The viscoelastic behavior can be easily understood if it is considered that these materials have properties common to elastic solids and viscous fluids, typically represented by springs and dashpots, respectively [3].

A simple example of viscoelastic behavior is the Maxwell model given by a spring (elastic behavior) and a dashpot (viscous behavior) placed in series [18] where Young's modulus function with time, known as the relaxation modulus, is given by:

$$E(t) = E_0 \exp(-t/\tau) \quad (1)$$

where E_0 is the glassy modulus ($t = 0$) and τ is the relaxation time that represents the ratio of viscosity to stiffness of the material [18].

In most practical materials, i.e. PVB, a more complex behaviour that that represented by Eq. (1) is expected, so that improved models such as the generalized Maxwell model must be used to adequately define the viscoelastic material behaviour. Usually the terms of the Maxwell model are rearranged in a Prony series [19] so that the relaxation modulus, $E(t)$, is given by the expression:

$$E_2(t) = E_0\left(1 - \sum_{i=1}^{n} e_i(1 - \exp(-t/\tau))\right) \quad (2)$$

where e_i and τ_i are the Prony series coefficients to be estimated for the viscoelastic material. Similar expressions can be directly obtained for the shear relaxation modulus, $G(t)$, that can also be calculated from the relaxation modulus by means of the viscoelastic correspondence principle [20, 21] using, e.g. the material bulk modulus, $K(t)$.

3 ANALYTICAL MODELS

Analytical models for triplex (glass+PVB+glass) laminated glass beams (Figure 1), usually consider the following assumptions:

- The mechanical behavior of glass is assumed to be linear-elastic whereas the PVB presents a homogeneous, isotropic, and linear-viscolelastic behavior (time and temperature dependent).
- The plane sections initially normal to the mid-surface in each glass ply remain plane and normal to the mid-surface during the bending. However, this property is not fulfilled for the entire beam.
- The transverse normal stress σ_z is small compared to the axial normal stress σ_x.
- The three layers have the same transversal displacement $w(x)$.
- No slip occurs at the interfaces between the glass and the PVB plies.
- The PVB-interlayer only transfers shear and has negligible compression in the transverse direction, i.e. $E_2^* \cong 0$.

3.1 The model of Koutsawa and Daya (KOU)

A model for laminated glass beams with two glass plies and a PVB interlayer on viscoelastic supports, which are modeled by two springs (rotational, K_R and translational K_T) on each end of the beam, was proposed by Koutsawa and Data [2].

The beam is subjected to distributed load q and to concentrated load P at the mid-point, and the origin of coordinate x is taken at the mid-point of the beam (Figure 1). The deflection of the beam under these loadings is given by:

$$w(x) = \frac{(\delta + \alpha^2\eta)f_1(x)}{\alpha^2} + \frac{f_2(x)}{24\alpha^2} \quad (3)$$

with

$$f_1(x) = a_3\cosh(\alpha x) + a_4\sinh(\alpha x) \quad (4)$$

$$f_2(x) = -q\delta\mu x^4 + 4\alpha^2\delta a_2 x^3 - 12(q\eta\mu - \alpha^2\delta a_1)x^2 + 24\alpha^2(a_5 x + a_6) \quad (5)$$

Where

$$\alpha = \sqrt{\frac{G_2^* b}{EH_2}\left(\frac{H_0^2}{I} + \frac{A_1 + A_3}{A_1 A_3}\right)} \quad (6)$$

$$\mu = \frac{G_2^* b H_0}{EIH_2} \quad (7)$$

and

$$I = I_1 + I_3 = \frac{b(H_1^3 + H_3^3)}{12}$$

$$\eta = \frac{H_2}{G_2^* b H_0}$$

$$\delta = -\left(\frac{A_1 + A_3}{A_1 A_3 E H_0}\right)$$

$$H_0 = \frac{H_1 + H_3}{2} + H_2$$

$$A_1 = bH_1$$

$$A_3 = bH_3$$

The six constants of integration a_1, a_2, a_3, a_4, a_5 and a_6 are determined using the boundary conditions and are listed in Appendix.

Using the shear parameter g and the geometric parameter Y, defined by Mead and Markus [22], DiTaranto [23] and Rao [24], i.e.:

$$Y = \frac{H_0^2}{I}\left(\frac{A_1 A_3}{A_1 + A_3}\right) \tag{8}$$

$$g = \frac{G_2^* b L^2}{4 E H_2}\left(\frac{A_1 + A_3}{A_1 A_3}\right) \tag{9}$$

the following alternative expressions are formulated for α and μ:

$$\alpha = \frac{2}{L}\sqrt{g(1+y)} \tag{10}$$

$$\mu = \frac{4gY}{H_0 L^2} \tag{11}$$

As regards the normal forces, it is fulfilled that $N_1 = -N_3$ [2], N_1 being given by:

$$N_1(x) = -\frac{q\mu x^2}{2\alpha^2} + a_1 + a_2 x + a_3 \cosh(\alpha x) + a_4 \sinh(\alpha x) \tag{12}$$

The stresses at the top and the bottom of glass plies are given as the summation of the contribution of normal forces and bending moments, i. e.:

$$\sigma_1^{top}(x) = \frac{N_1(x)}{bH_1} - \frac{EH_1}{2}w''(x) \quad (13)$$

$$\sigma_1^{bot}(x) = \frac{N_1(x)}{bH_1} + \frac{EH_1}{2}w''(x) \quad (14)$$

$$\sigma_3^{top}(x) = \frac{N_3(x)}{bH_3} - \frac{EH_3}{2}w''(x) \quad (15)$$

$$\sigma_{13}^{bot}(x) = \frac{N_3(x)}{bH_3} + \frac{EH_3}{2}w''(x) \quad (16)$$

3.1.1 Effective Thickness. Beam simply supported: distributed load.

These boundary and loading conditions are a particular case of the general model taking $K_R = 0$, $K_T = +\infty$ and $P = 0$.

The deflection at the mid-point of a laminated glass beam under distributed load can be derived from Eq. (3) taking $x = 0$, i.e.:

$$w(0) = \frac{q\mu}{\alpha^6}\left[(\delta + \alpha^2\eta)\frac{1}{\cosh\left(\frac{L\alpha}{2}\right)} + \frac{\Lambda_2}{384}\right] \quad (17)$$

As the goal is to determine the effective or equivalent monolithic bending stiffness $(EI)^*$, the following equation (equal bending deflection at the mid-span for both the monolithic and the laminated-glass beams) must be fulfilled, i.e.:

$$\frac{5qL^4}{384(EI)_q^*} = \frac{q\mu}{\alpha^6}\left[\frac{(\delta + \alpha^2\eta)}{\cosh\left(\frac{L\alpha}{2}\right)} + \frac{\Lambda_2}{384}\right] \quad (18)$$

From which:

$$(EI)_q^* = \frac{5L^4\alpha^6}{384\mu\left[\frac{(\delta+\alpha^2\eta)}{\cosh\left(\frac{L\alpha}{2}\right)}+\frac{\Lambda_2}{384}\right]} \tag{19}$$

Eq. (19) is the exact solution for the effective stiffness of a simply supported beam under distributed loading. Due to the fact that the shear modulus $G_2(t)$ is time (or frequency) and temperature dependent, also is the effective stiffness.

An effective thickness for deflection can be derived identifying the bending stiffness of a monolithic and a laminated-glass beam, i.e.:

$$E\frac{bH_{wq}^3}{12} = (EI)_q^* \tag{20}$$

from which:

$$H_{wq} = \sqrt[3]{\frac{60L^4\alpha^6}{384\mu bE\left(\frac{(\delta+\alpha^2\eta)}{\cosh\left(\frac{L\alpha}{2}\right)}+\frac{\Lambda_2}{384}\right)}} \tag{21}$$

This effective thickness is also time and temperature dependent.

It is important to remark that the effective thickness given by Eq. (21) corresponds to the deflection in the mid-span, in this case the maximum deflection. However, the effective thickness for any point of coordinate x_i in the beam can also be inferred taken $w(x_i)$ in Eq. (3).

With respect to the stresses, the maximum normal force in each glass ply is achieved at the mid-point of the beam, the top ply being in compression and the bottom ply in tensile. With regard to the bending moment, the maximum is also

achieved at the mid-point of the beam. Under the assumption that the vertical load is downwards, the stress on the top of the ply 1 is given by [2]:

$$\sigma_1^{top}(0) = \frac{N_1(0)}{bH_1} - \frac{EH_1}{2} w''(0) \tag{22}$$

where:

$$N_1(0) = \frac{q\mu}{2\alpha^2}\left[\frac{2}{\alpha^2 \cosh\left(\frac{L\alpha}{2}\right)} + \frac{L^2\alpha^2 - 8}{4\alpha^2}\right] \tag{23}$$

and

$$w''(0) = \frac{q\mu}{\alpha^6}\left[(\delta + \alpha^2\eta)\frac{\alpha^2}{\cosh\left(\frac{L\alpha}{2}\right)} + \frac{2\Lambda_1}{384}\right] \tag{24}$$

The effective thickness for stresses can be derived by identifying the bending stress of a monolithic and a laminated-glass beam, i.e.:

$$\frac{\frac{qL^2}{8}}{\frac{bH_{\sigma q}^2}{6}} = \frac{N_1(0)}{bH_1} - \frac{EH_1}{2} w''(0) \tag{25}$$

From Eq. (25), it is derived that:

$$H_{1\sigma q} = \sqrt[2]{\frac{8b}{6L^2\left(\frac{\frac{\mu}{2\alpha^2}\left(\frac{2}{\alpha^2\cosh\left(\frac{L\alpha}{2}\right)} + \frac{L^2\alpha^2-8}{4\alpha^2}\right)}{bH_1} + \frac{EH_1}{2}\frac{\mu}{\alpha^6}(\delta + \alpha^2\eta)\frac{\alpha^2}{\cosh\left(\frac{L\alpha}{2}\right)} + \frac{2\Lambda_1}{384}\right)}} \tag{26}$$

which is the effective thickness in bending for calculating stresses in ply 1. The effective thickness for ply 3 can be determined by following the same procedure and is given by:

$$H_{3\sigma q} = \sqrt[2]{\frac{8b}{6L^2\left(\frac{\frac{\mu}{2\alpha^2}\left(\frac{2}{\alpha^2\cosh\left(\frac{L\alpha}{2}\right)}+\frac{L^2\alpha^2-8}{4\alpha^2}\right)}{bH_3}+\right.}} \quad (27)$$
$$\left.+\frac{EH_3}{2}\frac{\mu}{\alpha^6}(\delta+\alpha^2\eta)\frac{\alpha^2}{\cosh\left(\frac{L\alpha}{2}\right)}+\frac{2\Lambda_1}{384}\right)$$

3.1.2. Effective thickness. Beam simply supported. Concentrated loading.

If the same procedure as that of the distributed loading is followed, taking $K_R = 0$, $K_T = +\infty$ and $q = 0$, it is derived that the effective stiffness is given by:

$$(EI)_P^* = \frac{EI\alpha^5\eta L^3}{48}\frac{1}{\left[(\delta+\alpha^2\eta)\left(\frac{L\alpha}{4}-\frac{\tanh\left(\frac{L\alpha}{2}\right)}{2}\right)-\frac{L^3\alpha^3}{48}\right]} \quad (28)$$

whereas the effective thickness for deflection is expressed as:

$$H_{wp} = \sqrt[3]{\frac{bI\alpha^5\eta L^3}{4\left[(\delta+\alpha^2\eta)\left(\frac{L\alpha}{4}-\frac{\tanh\left(\frac{L\alpha}{2}\right)}{2}\right)-\frac{L^3\alpha^3}{48}\right]}} \quad (29)$$

The effective thickness for stresses is given by:

$$H_{1\sigma p} = \sqrt[2]{\frac{4b}{6L\left(\frac{\frac{L}{4EI\alpha^2\eta}-\frac{L}{2EI\alpha^3\eta}\tanh\left(\frac{L\alpha}{2}\right)}{bH_1}+\right.}} \quad (30)$$
$$\left.+\frac{EH_1}{2}(\delta+\alpha^2\eta)\frac{PL}{2EI\alpha^3\eta}\tanh\left(\frac{L\alpha}{2}\right)+\frac{\delta PL}{4EI\alpha^2\eta}\right)$$

for ply 1, whereas the effective thickness for ply 3 is:

$$H_{3\sigma p} = \sqrt[2]{\frac{4b}{6L\left(\begin{array}{c}\dfrac{\frac{L}{4EI\alpha^2\eta} - \frac{L}{2EI\alpha^3\eta}\tanh\left(\frac{L\alpha}{2}\right)}{bH_3} + \\ + \frac{EH_3}{2}(\delta + \alpha^2\eta)\frac{PL}{2EI\alpha^3\eta}\tanh\left(\frac{L\alpha}{2}\right) + \frac{\delta PL}{4EI\alpha^2\eta}\end{array}\right)}} \tag{31}$$

3.1.3 Double-clamped beam.

A perfect clamped configuration is difficult to achieve in glass elements. In practical applications, fiber gaskets on both sides of the glass or similar devices are used to prevent the breakage of the glass. This means that the response of a laminated-glass beam in practice will vary between two limits: the simply supported and the double-clamped boundary configurations.

In the model of Koutsawa and Daya [2], the double-clamped configuration is a particular case of the general model taking $K_R = +\infty$ and $K_T = +\infty$. They assume the following boundary conditions for each extremity in the double-clamped configuration: $N = 0$, $w = 0$ and $w' = 0$.

Following the same procedure as in the simply supported case, the effective stiffness for a doubled-clamped beam under distributed loading is expressed as:

$$EI_q^* = \frac{qL^4}{384}\frac{1}{a_6 + a_3\frac{\delta + \alpha^2\eta}{\alpha^2}} \tag{32}$$

Whereas the expression for the concentrated load is given by:

$$EI_p^* = \frac{PL^3}{192}\frac{1}{a_6 + a_3\frac{\delta + \alpha^2\eta}{\alpha^2}} \tag{33}$$

The coefficients $a_3$and a_6 are listed in Appendix.

Eqs. (32) and (33) are used to derive the effective thickness for bending deflection, which is expressed as:

$$H_{wq} = \sqrt[3]{\frac{12}{Eb}\frac{qL^4\alpha^2}{384\ (\alpha^2 a_6 + a_3(\delta + \alpha^2\eta)}} \tag{34}$$

for distributed loading and

$$H_{wp} = \sqrt[3]{\frac{12}{Eb}\frac{PL^3\alpha^2}{192\ (\alpha^2 a_6 + a_3(\delta + \alpha^2\eta)}} \tag{35}$$

for concentrated loading.

With respect to the stress-effective thickness, this can be derived using the same procedure as in the simply supported case but no simple expressions can be formulated. The maximum stresses occur at the extremities of the beam and the stress-effective thicknesses at these points are determined from the equations:

$$\frac{\frac{qL^2}{12}}{\frac{bH_{1\sigma q}^2}{6}} = \frac{N\left(\frac{L}{2}\right)}{bH_1} - \frac{EH_1}{2}w''\left(\frac{L}{2}\right) \tag{36}$$

$$\frac{\frac{qL^2}{12}}{\frac{bH_{3\sigma q}^2}{6}} = \frac{-N\left(\frac{L}{2}\right)}{bH_3} + \frac{EH_3}{2}w''\left(\frac{L}{2}\right) \tag{37}$$

for the distributed load and from

$$\frac{\frac{PL}{8}}{bH_{1\sigma p}^2} = \frac{N\left(\frac{L}{2}\right)}{bH_1} - \frac{EH_1}{2}w''\left(\frac{L}{2}\right) \tag{38}$$

$$\frac{\frac{PL}{8}}{bH_{3\sigma p}^2} = \frac{-N\left(\frac{L}{2}\right)}{bH_3} + \frac{EH_3}{2}w''\left(\frac{L}{2}\right) \tag{39}$$

for the concentrated loading.

3.2 The model of Galuppi and Royer-Carfagni (GAL).

Recently, Galuppi and Royer-Cafagni [15], based upon a variational approach, have proposed a formulation for the effective thickness in laminated-glass beams, called Enhanced Effective Thickness method, which can be applied to a very wide range of boundary and loading conditions. Galuppi and Royer-Carfagni [15] have considered the deflection of the beam as:

$$w(x) = -\frac{g(x)}{EI^*} \tag{40}$$

where $g(x)$ is a shape function that takes the form of the elastic deflection of a monolithic beam with constant cross-section under the same loading and boundary conditions; I^* is a parameter representing the moment of the inertia of the laminated-glass beam given by:

$$\frac{1}{I^*} = \frac{\eta_g}{I_{tot}} + \frac{1-\eta_g}{I_1 + I_3} \tag{41}$$

The non-dimensional weight parameter η_g, which tunes the response from the layered limit ($\eta_g = 0$) to the monolithic limit ($\eta_g = 1$) is expressed as:

$$\eta_g = \frac{1}{1 + \frac{I_1 + I_3}{\mu_g I_{tot}} \frac{A_1 A_3}{A_1 + A_3} \psi} \tag{42}$$

where

$$\mu_g = \frac{\mathrm{G_2\ b}}{\mathrm{E\ H_2}} \tag{43}$$

$$I_{tot} = I_1 + I_3 + \frac{b H_1 H_3}{H_1 + H_3} H_0^2 \tag{44}$$

The parameter ψ depends on the boundary and loading conditions and is given by:

$$\Psi = \frac{\int_{-l/2}^{l/2} [g''(x)]^2 dx}{\int_{-l/2}^{l/2} [g'(x)]^2 dx} \tag{45}$$

The values for the most practical cases are tabulated in [17] and some of them reproduced in Table 1.

Then, the effective stiffness is given by:

$$EI^* = \frac{E}{\frac{\eta_g}{I_{tot}} + \frac{1 - \eta_g}{I_1 + I_3}} \tag{46}$$

Following the same procedure as in the previous section, the deflection effective thickness H_w is derived from Eq. 9 and turns out to be:

$$H_w = \sqrt[3]{\frac{1}{\frac{\eta_g}{(H_1^3 + H_3^3 + 12 I_s)} + \frac{(1 - \eta_g)}{(H_1^3 + H_3^3)}}} \tag{47}$$

where

$$I_s = \frac{H_1 H_3}{H_1 + H_3} H_0 \tag{48}$$

On the other hand, the stress-effective thicknesses are given by:

$$H_{1\sigma} = \sqrt{\frac{1}{\frac{2\eta_g H_{s2}}{H_1^3 + H_3^3 + 12I_s} + \frac{H_1}{H_w^3}}} \tag{49}$$

$$H_{3\sigma} = \sqrt{\frac{1}{\frac{2\eta_g H_{s1}}{H_1^3 + H_3^3 + 12I_s} + \frac{H_3}{H_w^3}}} \tag{50}$$

where

$$H_{s1} = \frac{h_1}{h_1 + h_3} H_0 \tag{51}$$

$$H_{s2} = \frac{h_3}{h_1 + h_3} H_0 \tag{52}$$

3.3 The model of Benisson et al. (BEN)

Benisson [12] was the first to propose an effective thickness, based on a previous work of Wölfel [14], for the calculation of laminated-glass elements. Wölfel [14] proposed a model for a sandwich structure composed of three layers, the external ones with considerable axial stiffness but negligible bending stiffness, while the intermediate layer can bear shear stress only with zero axial

and flexural strength. Bennison et al. [12] and Calderone et al. [13] have developed Wölfel's approach specifically for the case of laminated glass. This model assumes for the laminated-glass beam a deflection curve similar in type to the elastic curve of simply supported beam under uniformly distributed load and, consequently, turns out to be accurate when the case reflects these hypotheses. The validity of the method is limited because its simplifying assumptions are valid for statically determined composite beams, for which the bending stiffness of the composite plies is negligible. According to Bennison et al. [12] and Calderone et al. [13], the effective stiffness is given by the equation:

$$(EI)^* = EI(1 + \Gamma\mathrm{Y}) \tag{53}$$

where

$$\Gamma = \frac{1}{1+\gamma} \tag{54}$$

and

$$\gamma = \beta \frac{EH_1H_2H_3}{G_2^*(H_1+H_3)L^2} \tag{55}$$

β being a coefficient dependent on the boundary and loading conditions. Calderone et al. [13] and Bennison et al. [12] suggested to use $\beta = 9.6$ for any type of loading and boundary condition. However, Wölfel [14] proposed the $\beta = 9.6$ when the load is uniformly distributed; β = 12 for a concentrated force at midspan; $\beta = \pi^2$ for a sinusoidal load [14].

The effective thickness can be derived from Eq. (53) for the bending deflection, which is expressed as:

$$H_w = \sqrt[3]{\frac{12I(1+\Gamma Y)}{b}} \tag{56}$$

or alternatively:

$$H_w = \sqrt[3]{H_1^3 + H_3^3 + 12\Gamma\frac{H_0^2 H_1 H_3}{H_1 + H_3}} \tag{57}$$

Expressions similar to the one presented by Calderone et al. [13] (Eq. (56)) can be derived from Eqs. (28) and (33) expanding the hyperbolic cosine in Taylor series, i.e.:

$$\cosh\left(\frac{L\alpha}{2}\right) = 1 + \frac{L^2\alpha^2}{8} + \frac{L^4\alpha^4}{384} + \cdots \tag{58}$$

Considering two terms in Eq. (36), the effective stiffness becomes:

$$(EI)^* = EI\left(1 + \frac{Y}{1+\gamma+\frac{\gamma^2}{6(1+Y)-\gamma}}\right) \tag{59}$$

which is similar to the equation proposed by Calderone et al. [13].

With respect to the effective thickness for estimating stresses, it is given by:

$$H_{1\sigma} = \sqrt{\frac{H_{1w}^3}{H_1 + 2\Gamma\frac{H_0 H_3}{H_1 + H_3}}} \tag{60}$$

For ply 1 and by

$$H_{3\sigma} = \sqrt{\frac{H_{3w}^3}{H_3 + 2\Gamma\frac{H_0 H_3}{H_1 + H_3}}} \tag{61}$$

for ply 3.

4 CASE STUDIES

In this section, the accuracy provided by the models of Koutsawa and Daya (KOU), Galuppi and Royer-Carfagni (GAL) and Bennison et al. (BEN) are investigated. Laminated-glass beams with the following geometrical data have been considered in the simulations: $H_1 = 6$ mm, $H_3 = 4$ mm, $H_2 = 0.38$ mm, $b = 0.1$ m. The mechanical properties of glass and PVB described in section 5 were used in the simulations.

The effective thickness for bending deflection of a simply supported laminated glass beam under distributed loading and length $L = 1$ m, were estimated with the KOU, GAL and BEN models. Figure 2 shows that all the models provide the same effective thickness, with the discrepancies being less than 0.5%. Figure 3 presents the effective thickness for a shorter beam with $L = 0.2$ m. The errors are of the same order as those calculated for a longer beam (Figure 2).

In Figures 2 to 3, the borderlines (monolithic limit and the layered limit) of the effective thicknesses are indicated [15]. The maximum effective thickness coincides with the monolithic limit and occurs over the short term, whereas the minimum effective thickness occurs over the long term but do not always reach the layered limit. In Figure 3, corresponding to a short beam, it can be seen that the effective thickness has reached the layered limit but it is not the case for the long beam (Figure 2). For any set of thicknesses H_1, H_2 and H_3, it is inferred from Eq. (55) that the product $G_2 \cdot L^2$ (and not only G_2) determines the minimum effective thickness. Therefore, the minimum effective thickness never reaches the layered limit for a long beam.

With respect to the stress-effective thickness of a simply supported beam under distributed loading, all the models provide similar results, with the differences of less than 0.5%.

Very good agreement has also been found for the deflection-effective thickness of a simply supported beam under concentrated loading, being the differences less than 0.5%. With respect to the stress-effective thickness, the GAL and BEN models provide similar results being the error less than 2% (Figures 4 and 5). The discrepancies between the KOU model and the BEN and GAL models are close to 7% for H_1 and 2.5% for H_3 (see Figures 4 and 5).

Figure 6 shows the effective thickness for a double-clamped laminated-glass beam under distributed loading. Significant discrepancies were encountered between the models. The GAL and BEN models offer similar results over the short term (differences of less than 2%) but the differences increase with time, the maximum discrepancy being approximately 15%. The GAL and KOU models provide similar results over the long term but the maximum differences (c. 12%) occur over the short term.

5 EXPERIMENTAL TESTS

5.1 Material characterization

In this work, the glass mechanical properties were determined from static bending tests, from which a Young's modulus $E_1 = 72000$ MPa was estimated.

On the other hand, the experimental static characterization of PVB was made in a DMA RSA3 by subjecting PVB specimens with a thickness of 0.38 mm to 10 min of tensile relaxation tests. The PVB was tested at different temperatures from -15^oC to 50^oC in order to apply the Time-Temperature-Superposition

Principle (TTS) [3], for the construction of the PVB master curve. The TTS shift factors, a_T, were determined using the William, Landel and Ferry (WLF) model [4], i.e.:

$$\log(a_T) = -C_1 \frac{(T - T_0)}{C_2 + (T - T_0)} \quad (62)$$

where the coefficients $C_1 = 12.60$ and $C2 = 74.46$ were estimated for a reference temperature, $T_0 = 20^o C$, fitting all the experimental curves at different temperatures to Eq. (62). Once the experimental PVB relaxation master curve was established, the modulus was fitted with Eq. (2). The obtained Prony series coefficients are presented in Table 2. The Young's relaxation modulus, $E(t)$, together with the calculated shear relaxation modulus, $G_2(t)$ (assuming a constant bulk modulus of 2 GPa [5]) are presented in Figure 7.

5.2 Static bending tests.

Several experimental static tests were carried out on four laminated-glass beams under uniform distributed loading. Seven concentrated loads were used to reproduce this loading condition and the deflection at the mid-span was measured using a laser sensor.

5.2.1 Simply supported beams.

A simply supported beam with the following geometrical data: $H_1 = 3$ mm, $H_3 = 3$ mm, $H_2 = 0.38$ mm, $L = 1$ m and $b = 0.1$ m was tested for around 24 h under constant distributed loading $q = 19.7$ N/m at temperature $T = 17.5^o C$. A strain gauge was attached at the top of the glass ply of the beam to measure the strain at mid-span.

Figure 8 presents the experimental deflection together with the predictions by the GAL model, the error being less than 10%. Only the predictions with the GAL model are shown in the figures as the differences between the models are very small for this boundary condition.

The experimental stress at the mid-point of the beam (top ply), together with the analytical predictions, are presented in Figure 9. It can be observed that the analytical model predicts the stress with an error of less than 8%.

The same test was repeated at $T = 17.4^{o}C$ in a laminated-glass beam 1 m long and 0.1 m wide but with a non-symmetric layer configuration: $H_1 = 4$ mm, $H_2 = 0.38$ mm and $H_3 = 8$ mm. The loading was $q = 38.25$ N/m. Figure 10 shows that the analytical models predict the deflection of the beam with accuracy better than 9%.

With respect to the stress of the bottom glass ply at the mid-point, the differences between the experimental results and the predictions are less than 11% (see Figure 11).

For the effect of the thickness of the PVB layer to be considered, another test with the same boundary and loading configurations ($q = 38.25$ N/m) was performed in a beam with $L = 1$ m, $H_1 = 4$ mm, $H_2 = 0.76$ mm and $H_3 = 8$ mm at$T = 18.3^{o}C$. The results for the deflection, presented in Figure 12, shows very good agreement between the experimental results and the analytical prediction, the error being less than 2%.

5.2.2 Beam with three supports.

Finally, a laminated glass beam with the following data: $H_1 = 4$ mm, $H_2 = 4$ mm, $H_3 = 0.38$ mm, $L = 1.40$ m and $b = 0.1$ m was tested in three supports at $T = 17.8^o C$. The deflection and the strain were measured at the mid-point of one of the spams. The GAL model reproduces the experimental deflection with an error of less than 9%, and the stress with an error of less than 20% (see Figures 13 and 14, respectively).

Figure 14 reveals that the maximum stress at the top glass ply is reached at around $5 \cdot 10^4$ s and then diminishes, showing a trend different form the analytical prediction. This effect can also be seen in Figures 10 and 11. The temperature in the lab was not constant during the tests (slightly colder at night that at noon), and therefore the beam became slightly stiffer at lower temperatures, diminishing both the deflection and the stress.

6 CONCLUSIONS

In the last years, several analytical models have been proposed for the static analysis of laminated-glass beams. Koutsawa and Daya [2] proposed a model for laminated-glass beams supported by a viscoelastic material at the ends of the beam. This boundary condition is modeling by a translational spring K_T and a rotational spring K_R. The simply supported beam is a particular case of this model where it is assumed that $K_T = \infty$ and $K_R = 0$. On the other hand, the double-clamped configuration can be represented taking $K_T = \infty$ and $K_R = \infty$.

In most of the practical applications the laminated-glass elements are not entirely clamped. For example, windshields are usually fixed to the automobile frame with a viscoelastic material. In other applications such as balustrades, fiber gaskets are regularly used. The simply supported and the double clamped

cases can be considered as the two borderlines of the real support condition. The main strength of the KOU model is that any boundary condition can be modeled using appropriate stiffness for the springs K_R and K_T.

Bennison et al. [12] proposed the calculation of laminated-glass beams using the effective-thickness concept. This technique consists of calculating a thickness of a monolithic beam with equivalent bending properties to a laminated-glass beam. This methodology is very useful for engineers because the calculation of glass beams are significantly simplified, since the elastic bending formulas that employ this effective thickness can be used. The effective thickness is time and temperature dependent because the polymeric layer is also time and temperature dependent. The approach by Bennison et al. [12], based on the previous work of Wölfel [14], derives from assuming a deflection shape for the beam deformation similar to the elastic deflection of a simply supported beam under a uniformly distributed load [15].

Galuppi and Royer-Carfagni [15], using a variational approach, have recently proposed an alternative formulation for the effective thickness called the enhanced effective-thickness method, which can be applied to most loading and boundary conditions. In Galuppi and Royer-Carfagni [16] the methodology proposed in [15] has been extended to the two-dimensional case (laminated-glass plates), giving similar formulas to those corresponding to the one-dimensional case (beams). The main strength of the GAL model is that it can be applied to many loading and boundary conditions. All the equations and parameters needed for a quick calculation of laminated-glass beams using the effective-thickness concept are summarized by Galuppi et al. [17]. Compared with the Bennison approach [12], the equations are similar, they are easy to use

and, moreover, the Galuppi and Royer-Carfagni model [15] can be applied accurately to many more applications.

By simulations, as study was made of the accuracy achieved with the models of Koutsawa and Daya (KOU), Galuppi and Royer-Carfagni (GAL), and Calderone et al. (BEN). All the models provide similar results (errors of less than 1%) for the deflection- and stress-effective thickness of a simply supported beam under distributed loading. With respect to the simply supported beam under concentrated loading, the error was less than 2% for the deflection-effective thickness. Regarding the stress-effective thickness, the discrepancies between the GAL and BEN models are less than 2%, whereas the differences between the GAL and KOU model were close to 6%.

The maximum effective thickness coincides with the monolithic limit and occurs over the short term, whereas the minimum effective thickness occurs over the long term. The minimum effective thickness reaches the layered limit only for short beams because it depends on the product $G_2^* \cdot L^2$ (and not only on G_2). Therefore, the minimum effective thickness never reaches the layered limit for a long beam.

On the other hand, several experimental static tests were conducted on four laminated-glass beams under distributed loading in simply supported beams and with three supports, in order to validate the predictions of the analytical models. The analytical models predict the experimental deflection and the experimental stresses at the mid-point of the simply supported beams with an error less than 10%. Similar discrepancies exist for the deflection of the beam with three supports but a large error (≈ 20%) has been encountered for the stress predictions. However, it can be observed in Figures 8 to 14 that the

predictions are not always on the safe side. On the other hand, very good agreement was found between the experimental results and the analytical predictions for the beam with PVB thickness $H_2 = 0.76$ mm.

ACKNOWLEDGMENTS

The economic support given by the Spanish Ministry of Economy and Competitiveness through the projects BIA2008-06816-C02-01 and BIA2011-28380-C02-01 is gratefully appreciated.

REFERENCES

[1] Jones, D. Reflections on damping technology at the end of the twentieth century. J Sound Vib 1996; 190:449-462.

[2] Koutsawa, Y. and Daya, E. Static and free vibration analysis of laminated glass beam on viscoelastic supports. Int J Solids Struct 2007; 44:8735-8750.

[3] Ferry, J. Viscoelastic Properties of Polymers. Ltd. New York, 1980.

[4] Williams, M., Landel, R., and Ferry, J. The temperature dependence of relaxation mechanisms in amorphous polymers and other glass-forming liquids. J Am Chem Soc 1955; 77:3701-3707.

[5] Van Duser, A., Jagota, A., and Benninson, SJ. Analysis of glass/polyvinyl butyral laminates subjected to uniform pressure. J Eng Mech 1999; 125:435-442.

[6] Hooper, J. On the bending of architectural laminated glass. Int J Mech Sci 1973; 15:309-323.

[7] Behr, R., Minor, J., and Norville, H. Structural behavior of architectural laminated glass. J Struct Eng 1993; 119:202-222.

[8] Edel, M. The effect of temperature on the bending of laminated glass units. Ph.D. thesis, Texas A&M University, Department of Civil Engineering, College Station, Texas, 1997.

[9] Norville, H., King, K., and Swoord, J. Behavior and strength of laminated glass. J Eng Mech 1998; 124:46-53.

[10] Asik, M. and Tezcan, S. A mathematical model for the behavior of laminated glass beams. Comput Struct 2005; 83:1742-1753.

[11] Ivanov, I. Analysis, modeling and optimization of laminated glasses as plane beam. Int J Solids Struct 2006; 43:6887-6907.

[12] Benninson, SJ, Qin, MHX, and Davies, P. High-performance laminated glass for structurally efficient glazing. Innovative Light-weight Structures and Sustainable Facades, Hong Kong, May, 2008.

[13] Calderone, I., Davies, P., Bendat, J., and Bennison, SJ. Effective laminate thickness for the design of laminated glass. Glass Processing Days, Tampere, Finlandm, 2009.

[14] Wölfel, E. (1987) Nachgiebiger verbund eine näherungslösung und deren anwendungsmöglichkeiten. Stahlbau 1987; 6:173-180.

[15] Galuppi, L. and Royer-Carfagni, G. Effective thickness of laminated glass beams: New expression via a variational approach. Eng Struct 2012; 38:53-67.

[16] Galuppi, L. and Royer-Carfagni, G. The effective thickness of laminated glass plates. J Mech Mater Struct 2012; 7:375-400.

[17] Galuppi, L., Manara, G., and Royer-Carfagni, G. Practical expressions for the design of laminated glass. Composites: Part B 2013; 45: 1677-1688.

[18] Tschoegl, N. The Phenomenological Theory of Linear Viscoelastic Behavior: An Introduction. Springer-Verlag. Berlin, 1989.

[19] Tzikang, C. Determining a prony series for a viscoelastic material from time varyng strain data. NASA /TM-2000-210123, ARL-TR-2206, 2000.

[20] Read, W. Stress analysis for compressible viscoelastic materials. J Appl Phys 1950; 21:671-674.

[21] Lee, E. Stress analysis in viscoelastic bodies. Q J Mech Appl Math 1955; 21:671-674.

[22] Mead, D. and Markus, S. The forced vibration of three-layer damped sandwich beam with arbitrary boundary conditions. J Sound Vib 1969; 10:163-175.

[23] DiTaranto, R. and McGraw, J., Jr. Vibratory bending of damped laminated plates. J Eng Ind 1969; 91:1081-1090.

[24] Rao, D. Frequency and loss factors of sandwich beams under various boundary conditions. J Mech Eng Sci 1978; 20:271-282.

APPENDIX

$$a_1 = \frac{LP}{4EI\alpha^2\eta} + \frac{L^2 q\mu}{8\alpha^2} - \frac{Psinh\left(\frac{L\alpha}{2}\right)}{2EI\alpha^3\eta} + \frac{(C_1 + C_2)cosh\left(\frac{L\alpha}{2}\right)}{C_3}$$

$$a_2 = \frac{P}{2EI\alpha^2\eta}$$

$$a_3 = -\frac{(C_1 + C_2)}{C_3}$$

$$a_4 = \frac{P}{2EI\alpha^3\eta}$$

$$a_5 = -\frac{P(\delta + \alpha^2\eta)}{2EI\alpha^4\eta}$$

$$a_6 = -\frac{L^2 q(-5L^2\delta + 48\eta)\mu + g_1(a_3, a_4)}{348\alpha^2}$$

$$+ \frac{Lq\mu(-EI\delta + h_0) + g_2(a_3, a_4)}{2\alpha^2 K_T}$$

$$C_1 = -48(EI)^2 q\alpha^2\eta^2\mu + 24EIP\alpha^3\,\eta\,sinh\left(\frac{L\alpha}{2}\right) + (-24P\delta + 3L^2P\alpha^2\delta - 24P\alpha^2\eta + 2EIL^3q\alpha^2\delta\eta\mu)K_r$$

$$C_2 = -24(EILq\alpha^2\eta^2\mu K_r) + 24P\,\delta cosh\left(\frac{L\alpha}{2}\right)K_r + 24P\alpha^2\,\eta cosh\left(\frac{L\alpha}{2}\right)K_r - 12LP\alpha\delta\,sinh\left(\frac{L\alpha}{2}\right)$$

$$C_3 = 24EI\alpha^3\eta\left[(2EI\alpha^3\eta - L\alpha\delta K_r)cosh\left(\frac{L\alpha}{2}\right) + 2(\delta + \alpha^2\eta)K_r\,sinh\left(\frac{L\alpha}{2}\right)\right]$$

$$g_1(a_3, a_a) = 48[(-8 + L^2\alpha^2)\delta - 8\alpha^2\eta] + 16a_4\left[-(L^3\alpha^3\delta) + 12L\alpha(\delta + \alpha^2\eta) + 3\left((-8 + L^2\alpha^2)\delta - 8\alpha^2\eta\right)sinh\left(\frac{L\alpha}{2}\right)\right]$$

$$g_2(a_3, a_a) = 2\alpha^3\left[a_3(EI(\delta + \alpha^2\eta) - h_0)sinh\left(\frac{L\alpha}{2}\right) + a_4\left(-EI\delta + (EI(\delta + \alpha^2\eta) - h_0)cosh\left(\frac{L\alpha}{2}\right) + h_0\right)\right]$$

FIGURE CAPTIONS

Figure 1. Laminated-glass beam.

Figure 2. Simply supported beam under distributed loading. $H_1 = 6$ mm, $H_3 = 4$ mm, $H_2 = 0.38$ mm, $b = 0.1$ m, $L = 1$ m. a) Deflection-effective thickness with the KOU, GAL and BEN models. b) Mean square error.

Figure 3. Simply supported beam under distributed loading. $H_1 = 6$ mm, $H_3 = 4$ mm, $H_2 = 0.38$ mm, $b = 0.1$ m, $L =$1 m. a) Stress-effective thickness H_1 with the KOU, GAL and BEN models. b) Mean square error.

Figure 4. Simply supported beam under concentrated loading. $H_1 = 6$ mm, $H_3 = 4$ mm, $H_2 = 0.38$ mm, $b = 0.1$ m, $L =$1 m. a) Stress-effective thickness H_1 with the KOU, GAL and BEN models. b) Mean square error.

Figure 5. Simply supported beam under concentrated loading. $H_1 = 6$ mm, $H_3 = 4$ mm, $H_2 = 0.38$ mm, $b = 0.1$ m, L= 1m. a) Stress-effective thickness H_3 with the KOU, GAL and BEN models. b) Mean square error.

Figure 6. Double-clamped laminated-glass beam under distributed loading. $H_1 = 6$ mm, $H_3 = 4$ mm, $H_2 = 0.38$ mm, $b = 0.1$ m, $L =$1 m. a) Deflection-effective thickness with the KOU, GAL, and BEN models. b) Mean square error.

Figure 7. Tensile and shear relaxation moduli of PVB at $T = 20^oC$.

Figure 8. Deflection of a simply supported beam under distributed loading. $H_1 = 3$ mm, $H_3 = 3$ mm, $H_2 = 0.38$ mm, $L = 1$ m, $b = 0.1$ m, $q = 19.7$ N/m and $T = 17.5^oC$.

Figure 9. Maximum stress at the mid-point of the top glass ply. Simply supported beam under distributed loading. $H_1 = 3$ mm, $H_3 = 3$ mm, $H_2 = 0.38$ mm, $L = 1$ m, $b = 0.1$ m, $q = 19.7$ N/m and $T = 17.5^oC$.

Figure 10. Deflection of a simply supported beam under distributed loading. $H_1 = 4$ mm, $H_3 = 8$ mm, $H_2 = 0.38$ mm, $L = 1$ m, $b = 0.1$ m, $q = 38.25$ N/m and $T = 17.4^oC$.

Figure 11. Maximum stress at the mid-point of the bottom glas ply. Simply supported beam under distributed loading. $H_1 = 4$ mm, $H_3 = 8$ mm, $H_2 = 0.38$ mm, $L = 1$ m, $b = 0.1$ m, $q = 38.25$ N/m and $T = 17.54^oC$.

Figure 12 Deflection of a simply supported beam under distributed loading. $H_1 = 4$ mm, $H_3 = 8$ mm, $H_2 = 0.76$ mm, $L = 1$ m, $b = 0.1$ m, $q = 38.25$ N/m and $T = 18.3^oC$.

Figure 13. Deflection of a beam with three supports under distributed loading. $H_1 = 4$ mm, $H_3 = 4$ mm, $H_2 = 0.38$ mm, $L = 1.4$ m, $b = 0.1$ m, $q = 94.22$ N/m and $T = 17.8^oC$.

Figure 14. Maximun stress at the mid-point of the top glass ply. Beam with three supports under distributed loading. $H_1 = 4$ mm, $H_3 = 4$ mm, $H_2 = 0.38$ mm, $L = 1.4$ m, $b = 0.1$ m, $q = 94.22$ N/m and $T = 17.8^oC$.

TABLE CAPTIONS

Table 1. Coupling parameter ψ for laminated-glass beams.

Table 2. Prony series coefficients for PVB.

Table1

Click here to download Table: Table1.docx

Boundary conditions	Loading	
Simply supported	Distributed	——
Simply supported	Concentrated mid-point	—
Double clamped	Distributed	—
Three supports	Distributed	—
Clamped-simply	Distributed	—

Table2

Click here to download Table: Table2.docx

[s]	
2.36600000000000E-07	2.342151953E-01
2.26430000000000E-06	2.137793134E-01
2.16668000000000E-05	1.745500419E-01
2.07327300000000E-04	1.195345045E-01
1.98389580000000E-03	1.362133454E-01
1.89837195000000E-02	6.840656310E-02
1.81653498300000E-01	4.143944180E-02
1.73822593210000E+00	7.251952800E-03
1.66329270788000E+01	2.825459600E-03
1.59158978189400E+02	2.712854000E-04
1.52297789909670E+03	4.293523000E-04
1.45732380763177E+04	9.804730000E-05
1.39449999999999E+05	5.274937000E-04

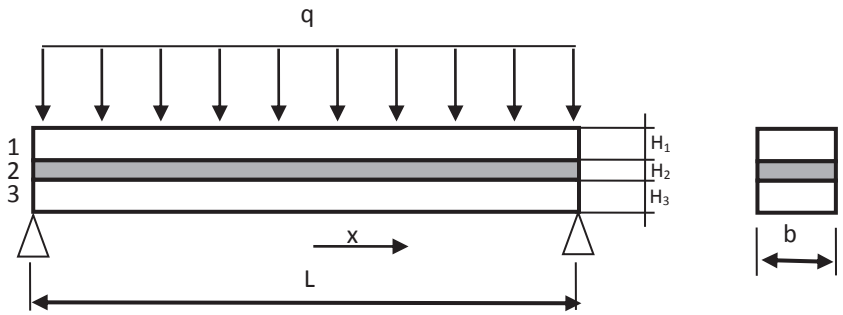
q
1
2
3
H1
H2
H3
x
L
b

Figure2
Click here to download Figure: Figure2.eps

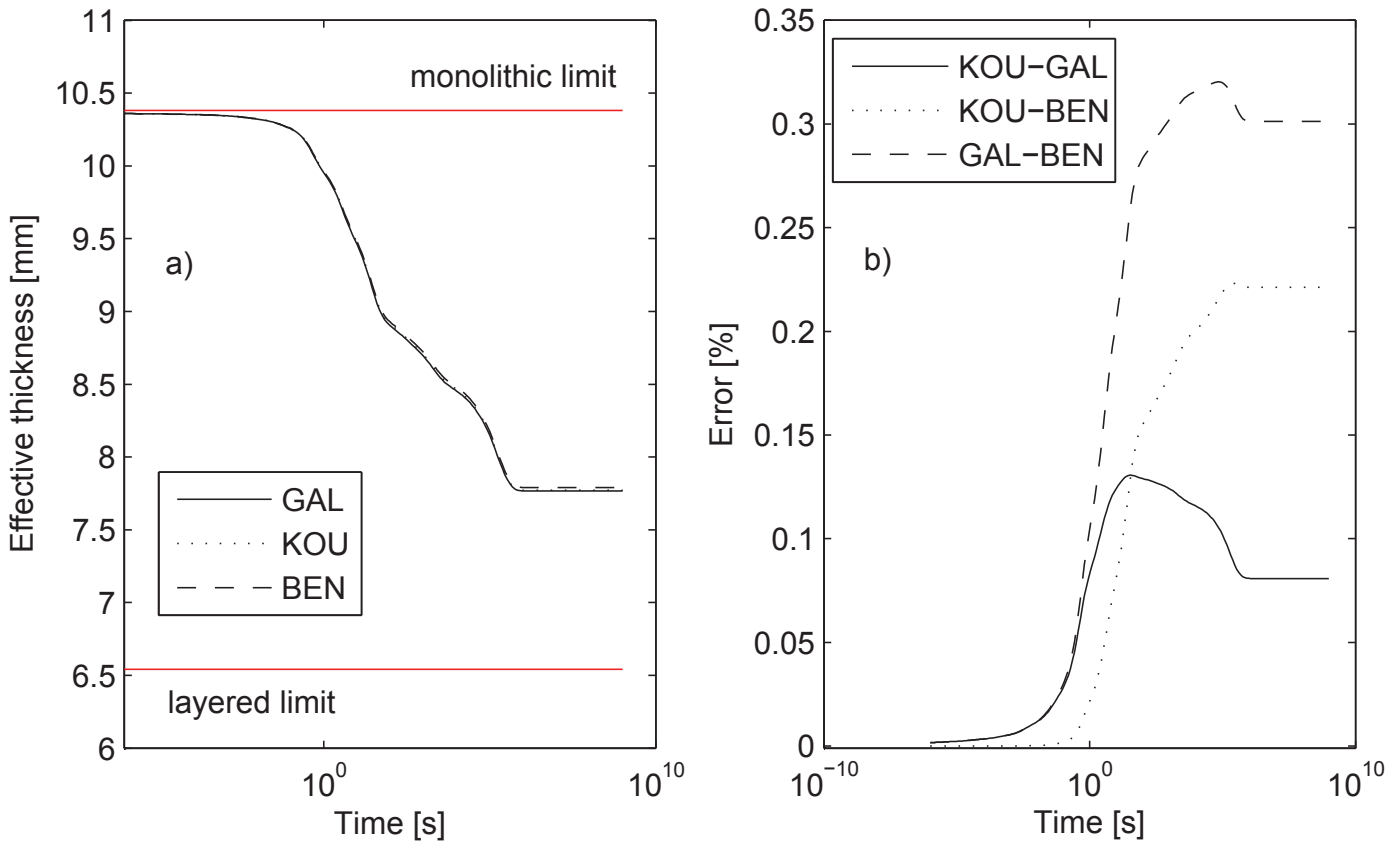

Figure3
Click here to download Figure: Figure3.eps

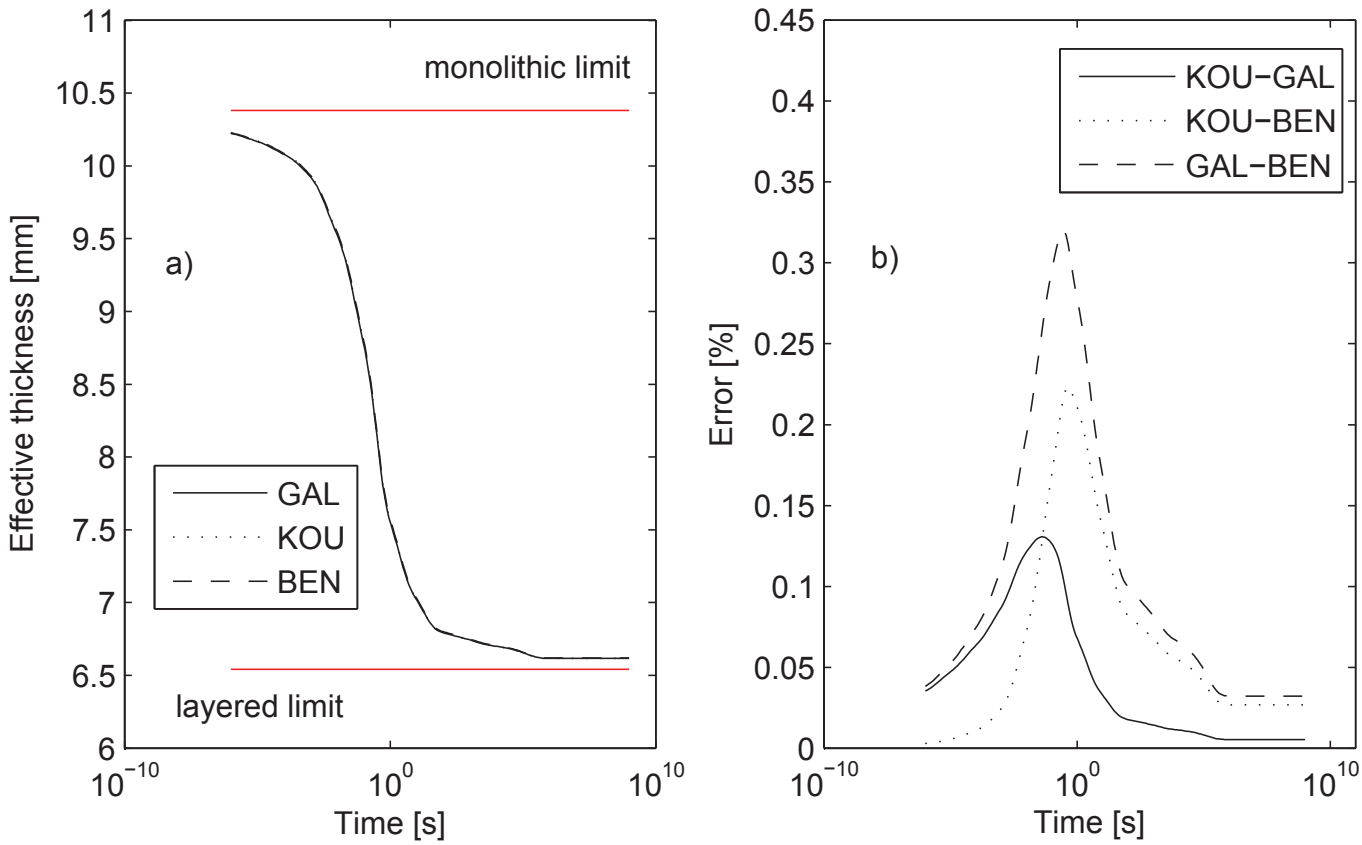

Figure4
Click here to download Figure: Figure4.eps

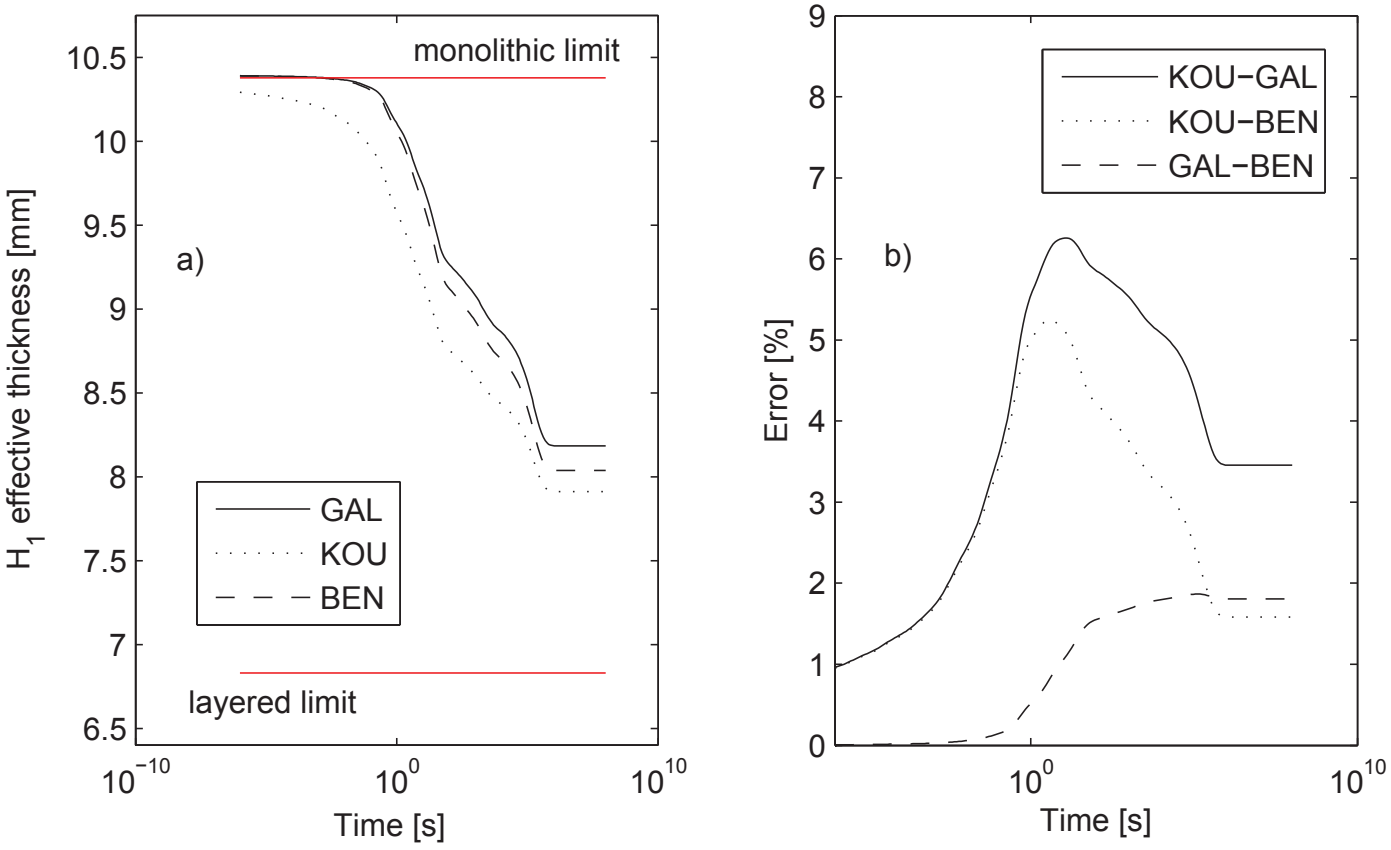

Figure5
Click here to download Figure: Figure5.eps

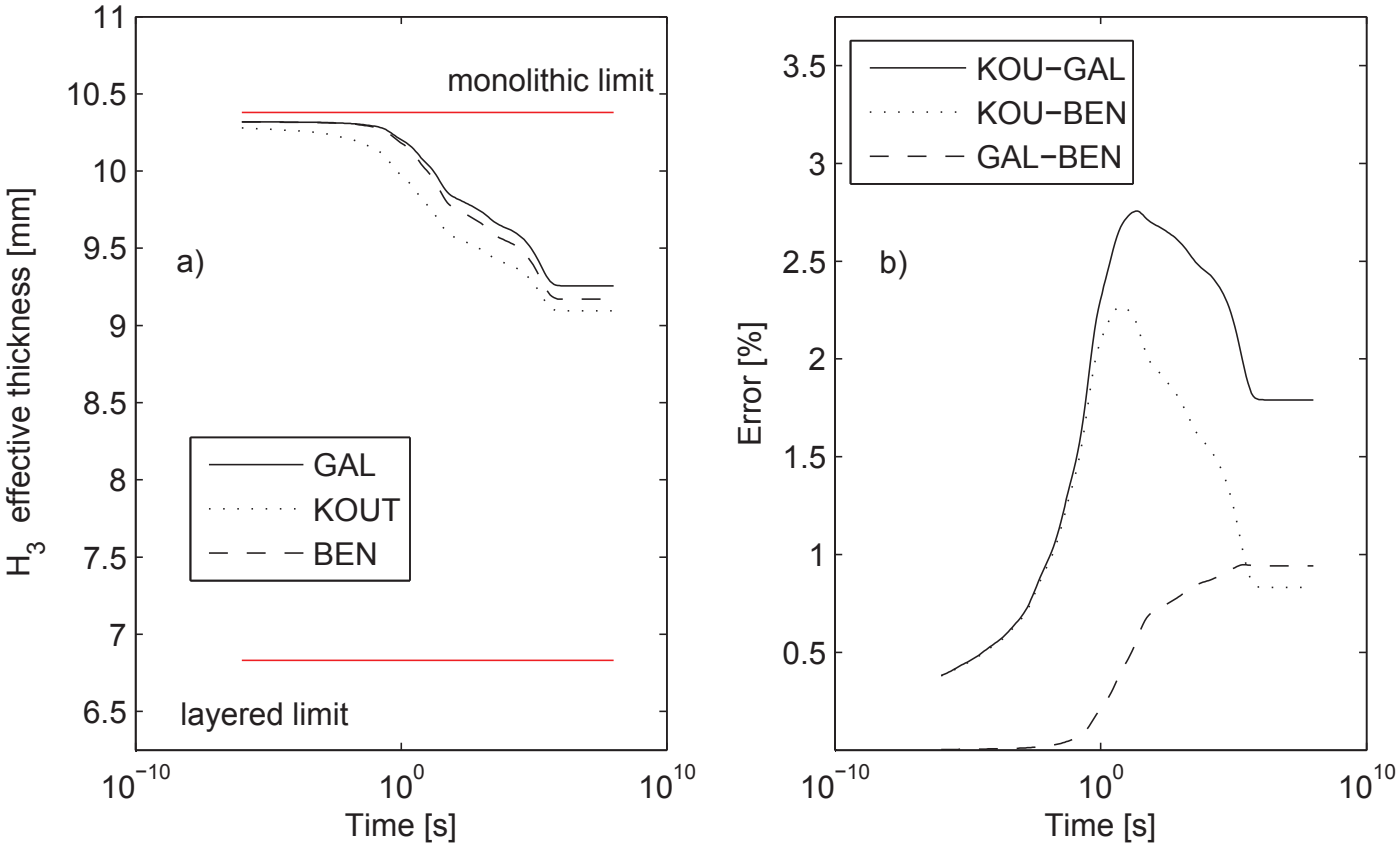

Figure6
Click here to download Figure: Figure6.eps

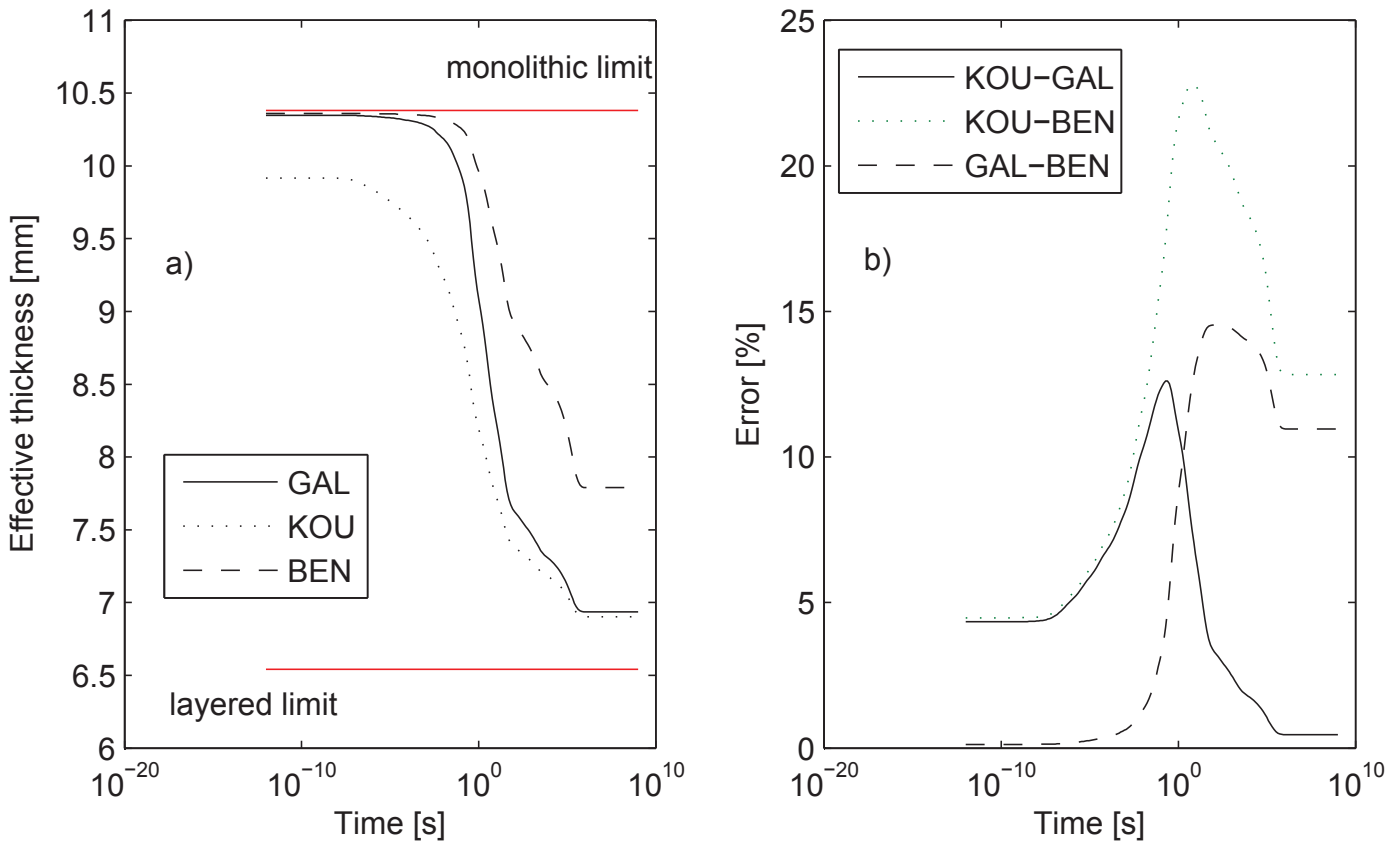

Figure7
Click here to download Figure: Figure7.eps

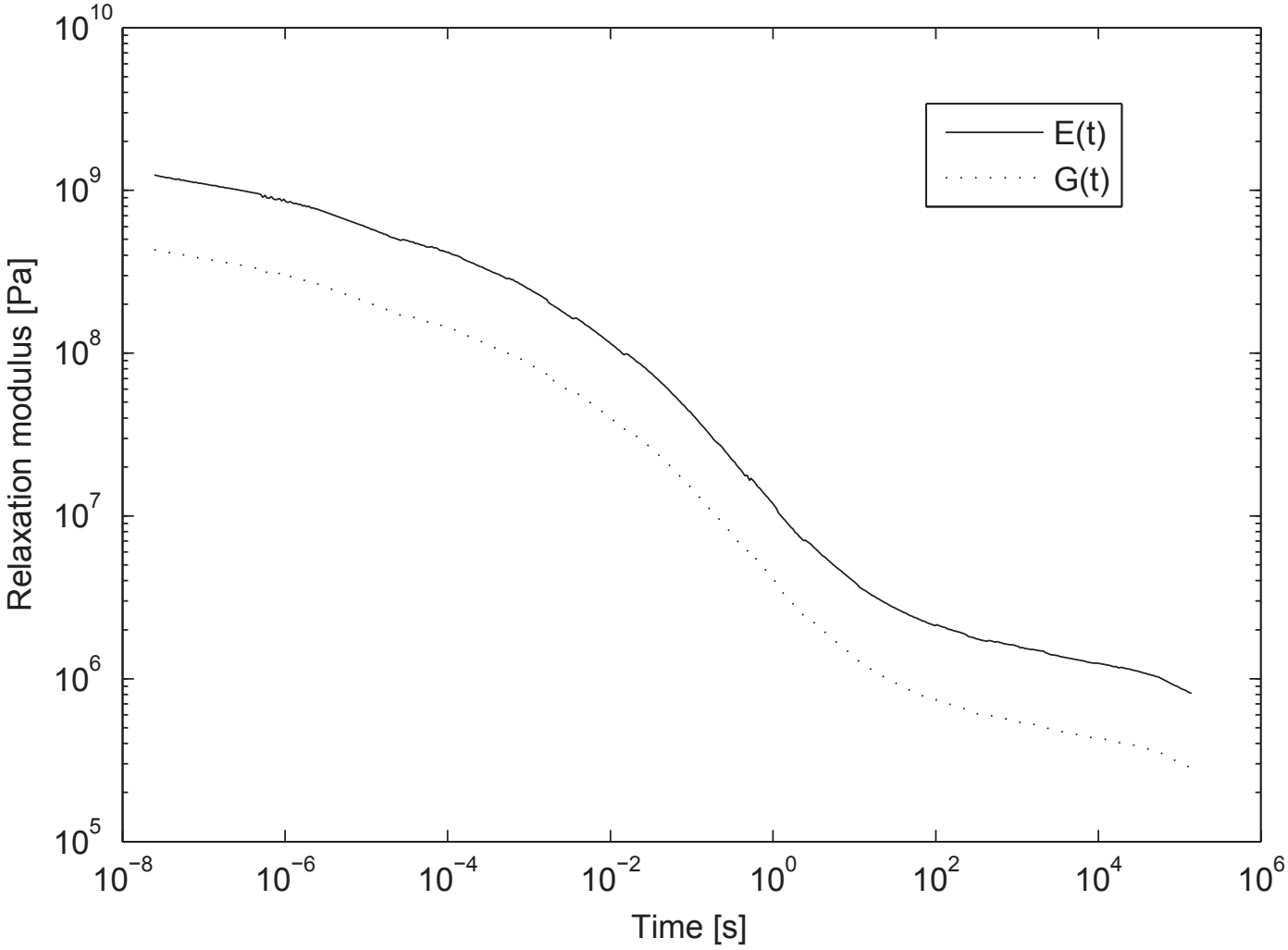

Figure8
Click here to download Figure: Figure8.eps

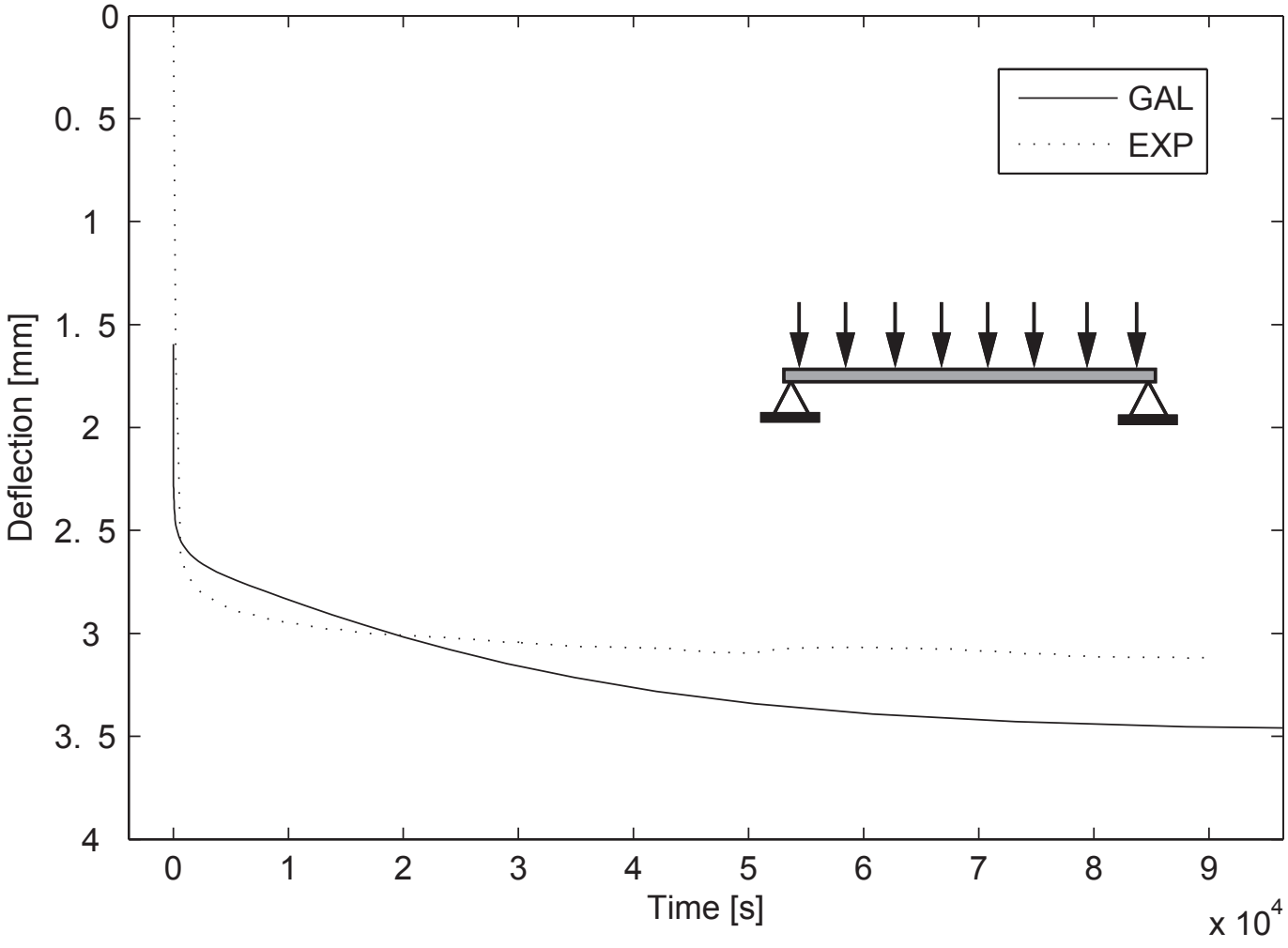

Figure9
Click here to download Figure: Figure9.eps

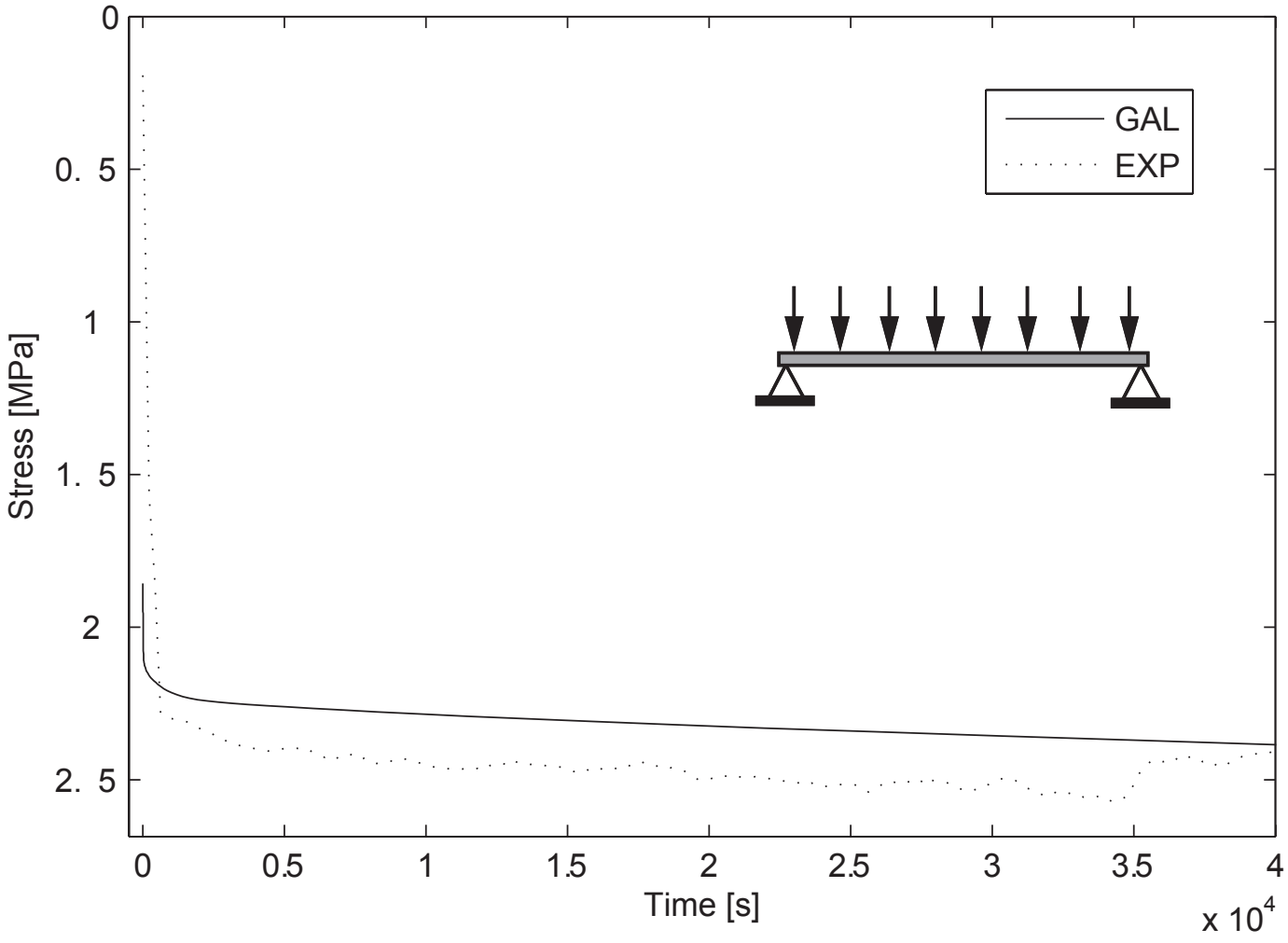

Figure10
Click here to download Figure: Figure10.eps

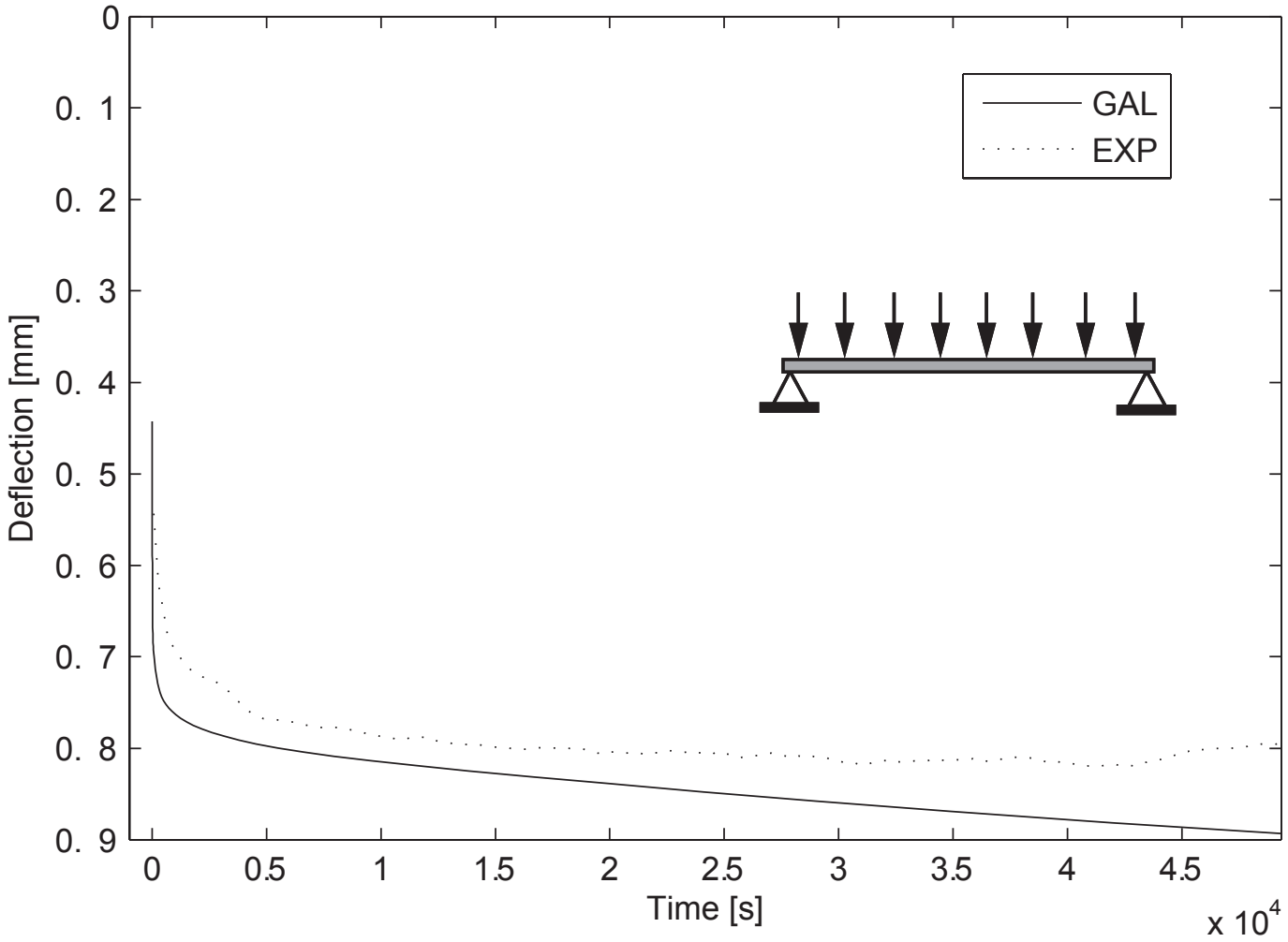

Figure11
Click here to download Figure: Figure11.eps

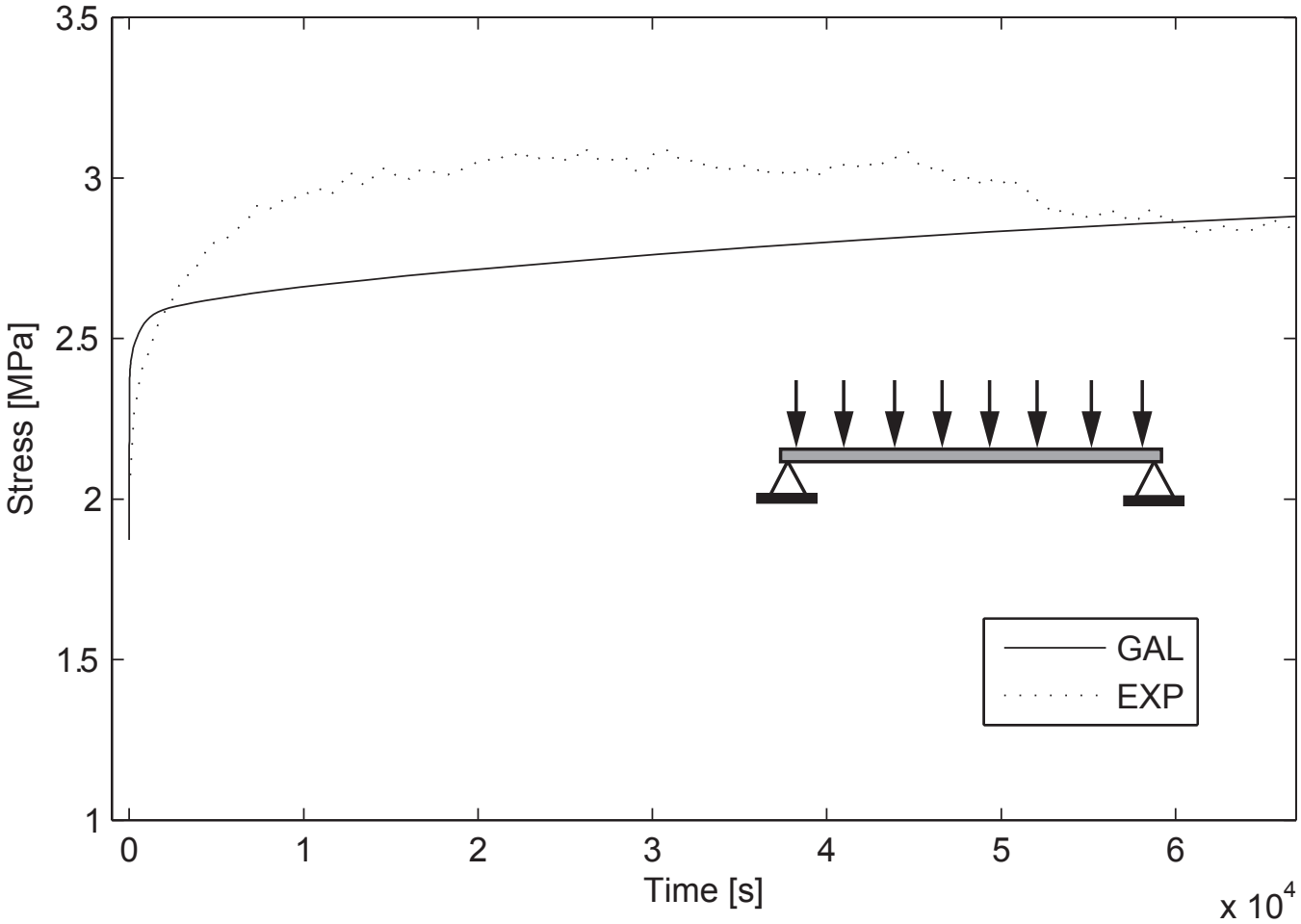

Figure12
Click here to download Figure: Figure12.eps

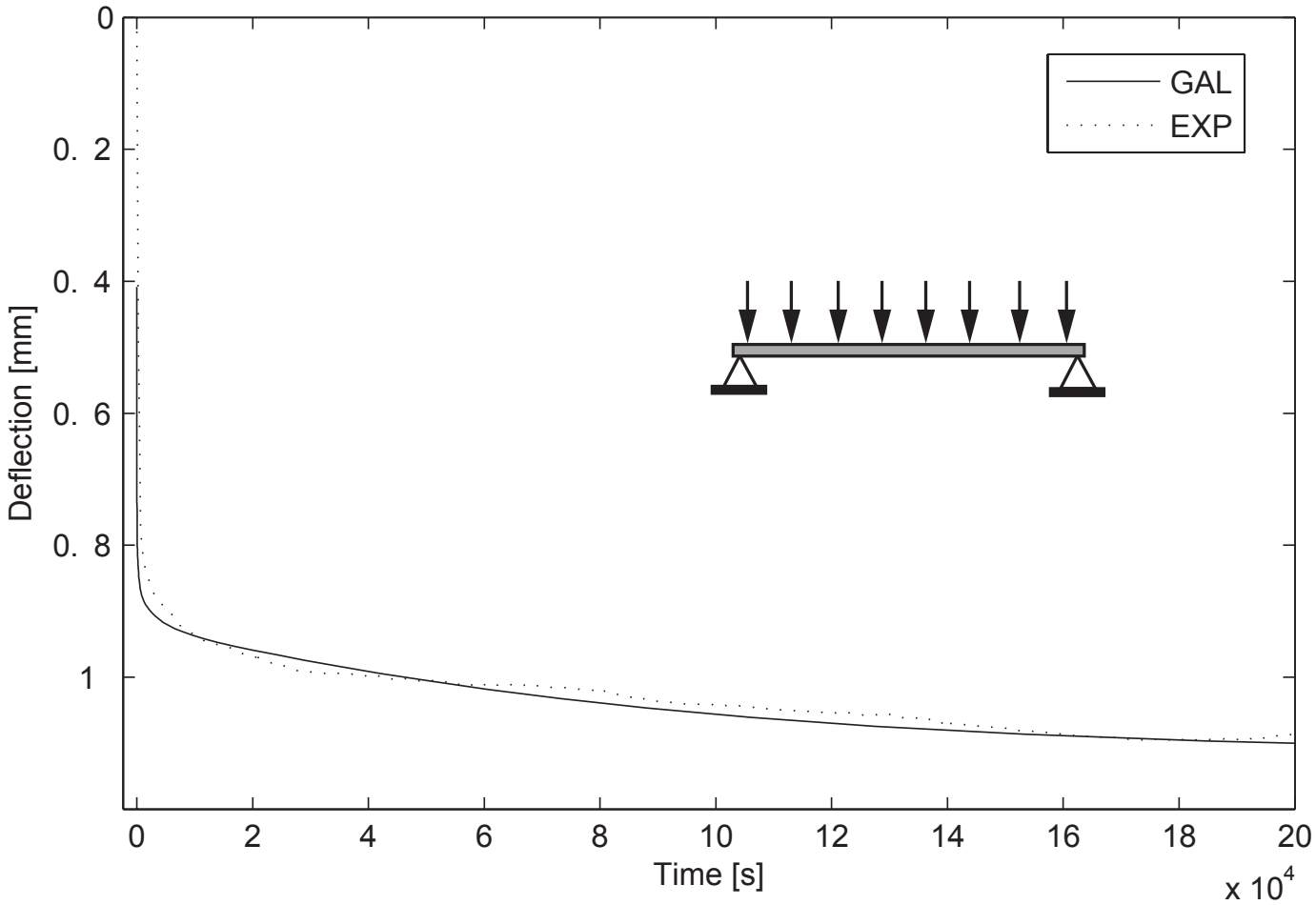

Figure13
Click here to download Figure: Figure13.eps

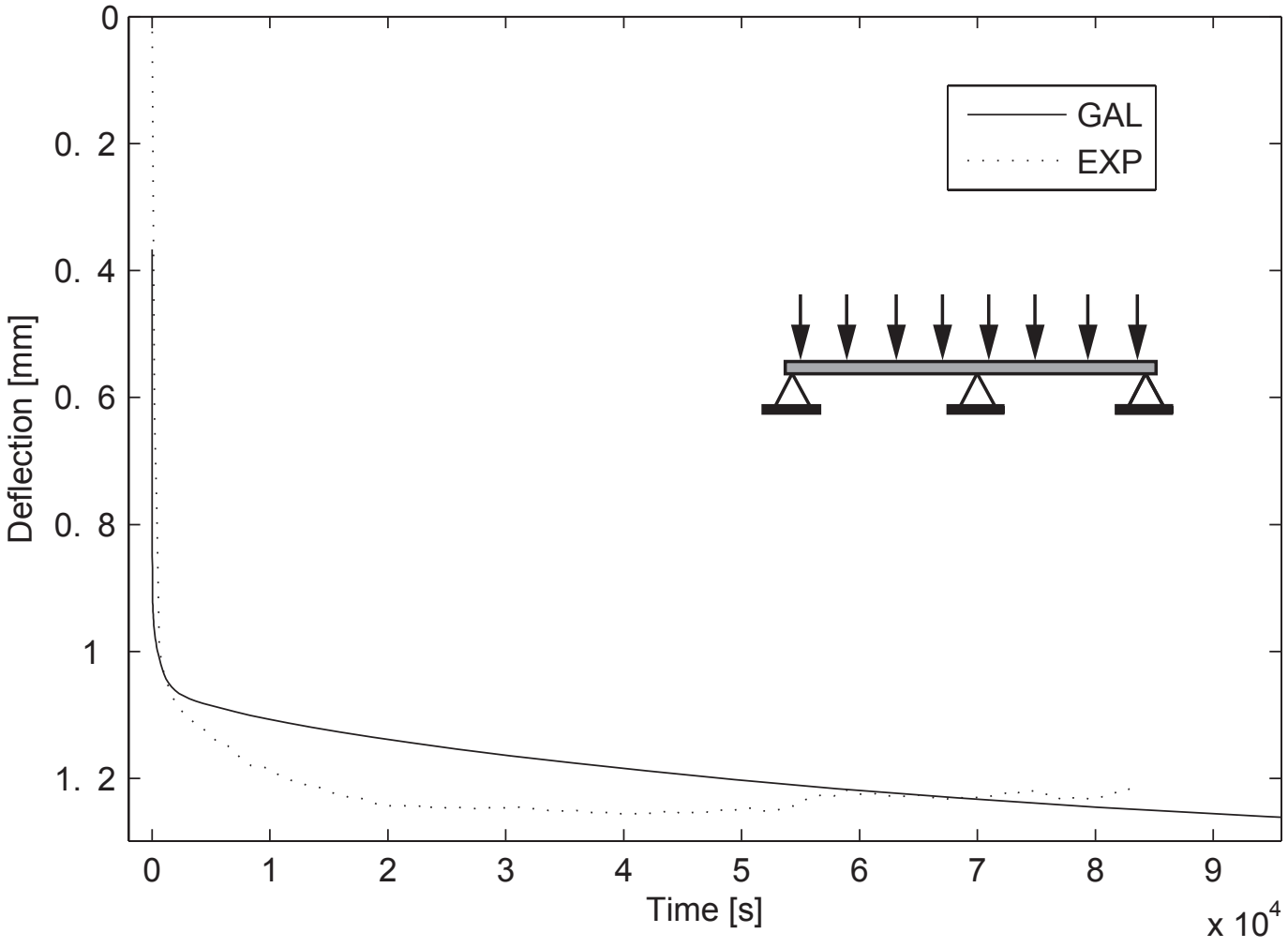

Figure14
Click here to download Figure: Figure14.eps

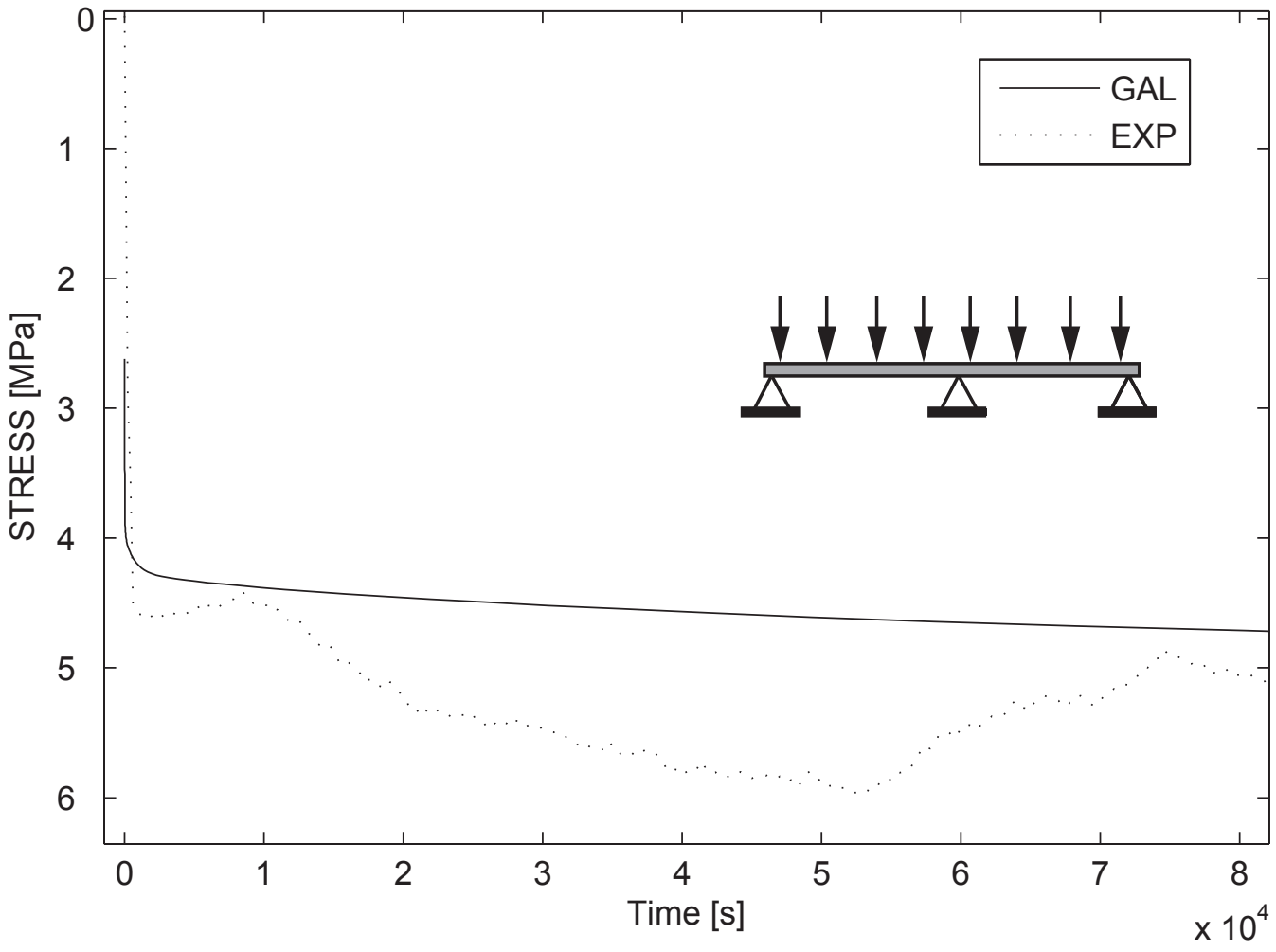

Original Word Document

Click here to download Supplementary Material for on-line publication only: EffectiveThicknessConcept.docx